COBEM 2023 27TH INTERNATIONAL CONGRESS OF MECHANICAL ENGENEERING

ABCM Brazilian Society of Mechanical Sciences and Engineering
27th ABCM International Congress of Mechanical Engineering
December 04-08, 2023, Florianópolis-SC, Brazil

COB-2023-0963
Boundary integral simulations based on the vortex-sheet formalism for the discretization of sharp droplet interfaces in Hele-Shaw cells

Rafael M. Oliveira
Departamento de Engenharia Mecânica, Pontifícia Universidade Católica do Rio de Janeiro, Rio de Janeiro RJ 22451-900, Brazil
rmo@puc-rio.br

Abstract. *We track nonlinear deformations of liquid droplets confined in the parallel plates of a Hele-Shaw cell surrounded by a fluid of different viscosity. For that purpose, we apply an accurate boundary integral method based on the vortex-sheet formalism, which measures the jump of the tangential component of velocity as one crosses the interface. Because of Darcy's law, the interior and exterior fluids are potential, and the bulk of both fluids is irrotational, making vorticity to be concentrated at the sharp interface between them. In addition, because of sharpness, the vortex-sheet becomes a quantity better suited to access information regarding vorticity. It is defined at the interface between the fluids and is used to track the nonlinear deformations. The plane curve that describes the interface is constrained by surface tension and evolves according to its normal velocity, which depends on the vortex-sheet distribution. So, the vortex-sheet is used to describe the morphology of the interfacial patterns and needs to be calculated in every time step. In the current work, we discuss this methodology and present results of different Hele-Shaw flow configurations, including (i) Growth of viscous fingers by radial injection; (ii) Fingering formation driven by centrifugal effects in rotating Hele-Shaw cells; and (iii) Deformations of magnetic droplets subjected to different external magnetic fields.*

Keywords: *Fingering instability, Hele-Shaw cell, Boundary-integral method, Vortex-sheet formalism, Magnetic fluids*

1. INTRODUCTION

Displacements between the parallel plates of a Hele-Shaw cell have become a paradigm for studying hydrodynamic instabilities and pattern formation in two-phase flows (Homsy, 1987; McCould and Maher, 1995; Casademunt, 2004). A classical example is the Saffman-Taylor problem and formation of branched viscous fingering patterns when a viscous fluid is displaced by a less viscous one (Saffman and Taylor, 1958). Investigations in non-standard Hele-Shaw configurations have also attracted increased interest (Morrow *et al.*, 2019). These include Hele-Shaw cells with variable permeability given by gap gradients and displacements driven by centrifugal effects when the Hele-Shaw cell is rotated. Other variations include displacements of non-Newtonian and magnetic fluids (Oliveira and Miranda, 2020; Oliveira *et al.*, 2021; Abedi *et al.*, 2022). In all cases, the internal fluid, given by the injected invading fluid or by a droplet of constant volume, deforms the immiscible interface between both phases giving rise to striking interfacial patterns.

This works describes a highly accurate numerical approach that is employed to simulate the fully nonlinear interface deformations in problems that are dominated by the action of surface tension: The boundary integral method based on the vortex-sheet formalism (Hou *et al.*, 1994; Ceniceros *et al.*, 1999; Hou *et al.*, 2001; Oliveira and Miranda, 2020; Oliveira *et al.*, 2021, 2023). The confined geometry of the Hele-Shaw cell allows derivation of generalized Darcy's laws to govern the evolution of each fluid. This simplified momentum equation states that velocity is proportional to the gradient of a generalized pressure, which makes the bulk velocity of each fluid irrotational. In addition, moving boundary conditions need to be specified at the sharp interface that separates both phases. These are usually given by a pressure jump boundary condition and by the kinematic condition, which specifies continuity of the normal component of the fluids velocities as one crosses the interface. However, the tangential velocity component is discontinuous at the interface making vorticity to concentrate at this location. Furthermore, because the interface is described by a sharp planar curve, the vortex sheet becomes a quantity better suited to access the locations where vorticity is concentrated and the position of the interface itselt. This quantity explores the jump in the tangential velocity components of the fluids.

The following sections presents the governing equations and the boundary integral method giving an emphasis on how evolution equations are coupled to the description of nonlocal distribution of vortex sheet. Then, to illustrate method capabilities, we present a few results of selected Hele-Shaw displacement flows and point the interested reader to complete works for detailed physical discussion of each particular problem. The results presented address: (i) Displacements of a Newtonian fluid by radial injection; (ii) Pattern formation in centrifugally-driven flows; and (iii) Deformations of magnetic droplets subjected to different magnetic field configurations.

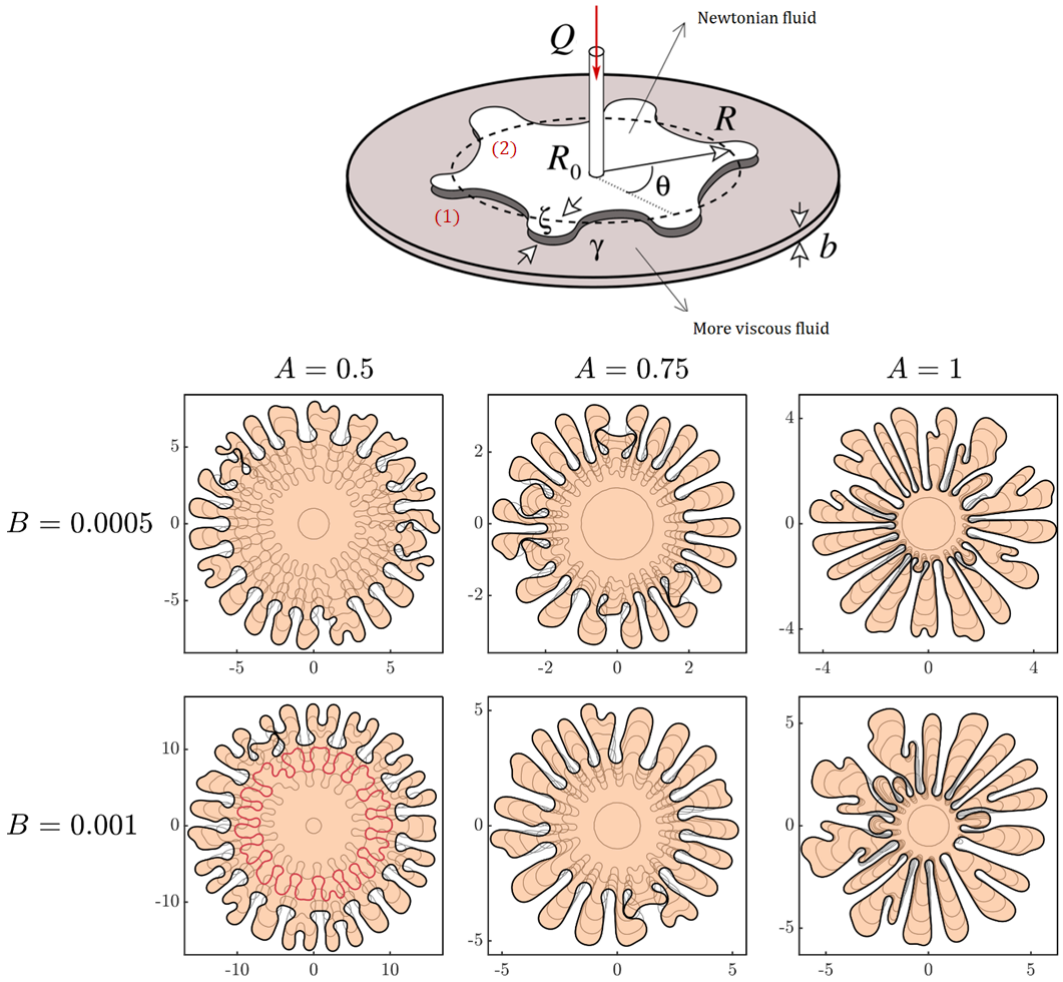

Figure 1. Schematic figure and simulation results showing the growth of viscous fingering by the radial injection of a less viscous fluid.

2. GOVERNING EQUATIONS AND THE VORTEX SHEET FORMALISM

We investigate the interfacial deformations of droplets confined in a Hele-Shaw cell. The trapped fluid can be Newtonian, non-Newtonian or magnetic and it is surrounded by an external fluid that is Newtonian and immiscible with the droplet. Different physical systems are considered and the driving mechanism of instability differs from case to case. Examples of destabilizing mechanisms include the radial injection of a less viscous fluid, centrifugal effects when the Hele-Shaw cell is rotated, or a magnetic field that tends to stretch magnetic droplets. In all cases, surface tension has a strong influence on pattern formation, having a stabilizing effect on interface perturbations. Surface tension arises in the modeling by applying the Young-Laplace boundary condition at the interface between the fluids,

$$p_2 - p_1 = \sigma\kappa, \tag{1}$$

where p_1 (p_2) is the pressure at the external (internal) fluid, σ is the surface tension, and κ is the in-plane curvature. Curvature introduces terms that have a large number of spatial derivatives, which induces constraint on time-step integration. This may lead to numerical stiffness and motivates application of the Frenet-Serret identity

$$\kappa = \theta_s = \frac{\theta_\alpha}{s_\alpha}, \tag{2}$$

where θ is the tangent angle, s is the arclength, and α is a parameter that parameterizes the planar curve that describes the interface. Subscripts indicate partial differentiation. The numerical integration method applied in the current work focuses on the discretization of this term as will be described below. This integration method has been used by a few authors, including Hou *et al.* (1994, 2001); Miranda and Alvarez-Lacalle (2005); Alvarez-Lacalle *et al.* (2006); Zhao *et al.* (2020); Oliveira and Miranda (2020); Oliveira *et al.* (2021, 2023).

Evolution equations to determine the shape of the interface can be written in terms of the tangent angle, θ, and local

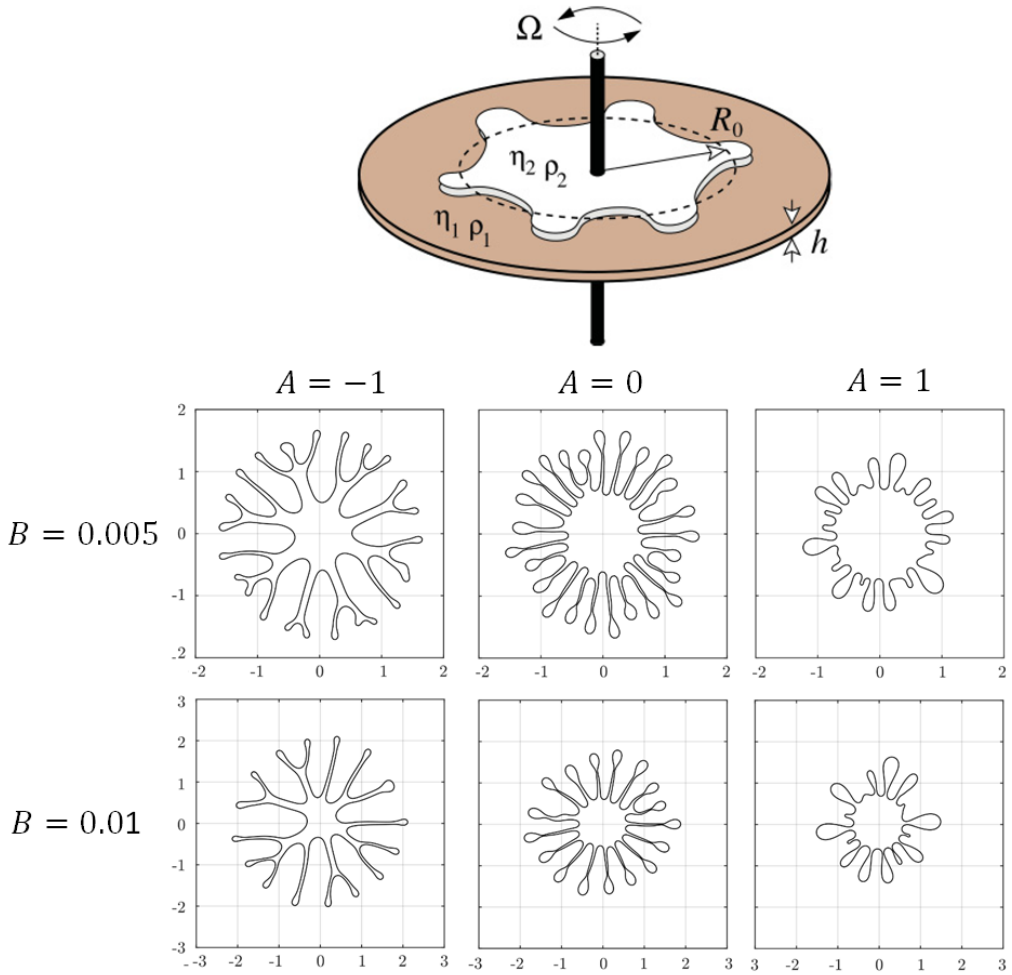

Figure 2. Schematic figure and simulation results for showing interfacial patterns growing under the influece of centrifugal effects.

arclength derivatives, s_α. These can be obtained from

$$\mathbf{X}_t = U\hat{n} + T\hat{s}, \tag{3}$$

where

$$\mathbf{X}(\alpha, t) = (x(\alpha, t), y(\alpha, t)) = r(\alpha, t)(\cos\varphi(\alpha, t), \sin\varphi(\alpha, t)) \tag{4}$$

describes the interface position parameterized by α that evolves in time, t. The normal (tangent) component of the interface velocity is given by U (T). These quantities will be obtained by considering governing equations in the form of a generalized form of Darcy's law suited for each particular Hele-Shaw displacement flow alongside interface boundary conditions, the pressure-jump boundary condition (Eq. 1) and a kinematic boundary condition that specifies continuity of the normal component of the fluids velocities as one crosses the interface. In addition, to obtain evolution equations in terms of θ_α and s_α, we require the unit tangent angle, which is written as

$$\hat{s} = \frac{1}{s_\alpha}(x_\alpha, y_\alpha) = (\cos\theta, \sin\theta). \tag{5}$$

By taking the partial derivative in α of Eq. (3) and matching with Eq. (5) after differentiating in time, one finds

$$s_{\alpha,t} = T_\alpha - U\theta_\alpha, \tag{6}$$

$$\theta_t = \frac{1}{s_\alpha}(U_\alpha + T\theta_\alpha). \tag{7}$$

To make this set of Eqs. (6) and (7) complete in the description of the evolution of the interface, we need to couple the normal interface velocity, U, and the tangent interface velocity, T, with the governing equations and boundary conditions.

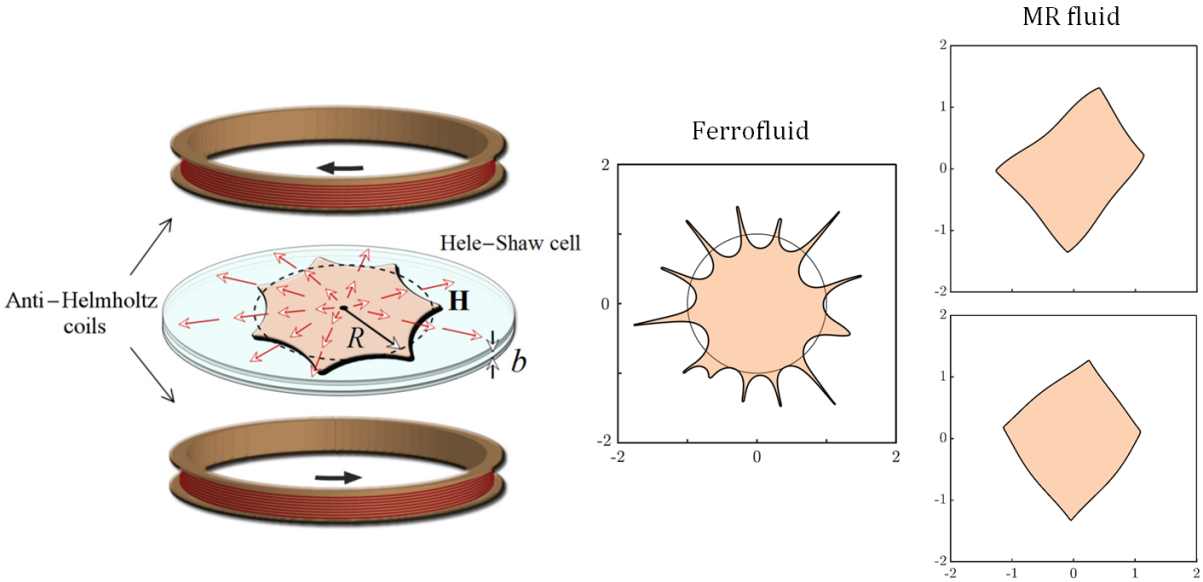

Figure 3. Ferrofluid and magnetorheological fluid are radially stretcheed under the influence of a magnetic field generated by two coils in the anti-Helmholtz configuration.

For radial displacements by injection of a less viscous fluid and the formation of viscous fingering instabilities (cf. Fig. 1), the momentum equations is given by the standard Darcy's law for a Hele-Shaw cell,

$$\boldsymbol{u}_i = -\frac{b^2}{12\eta_i}\nabla p_i, \tag{8}$$

where $\boldsymbol{u}_1$ ($\boldsymbol{u}_2$) denotes the velocity, $p_1(p_2)$ captures the pressure for the external (internal) fluid, and b denotes the gap thickness of the Hele-Shaw cell. The vortex sheet, $\tilde{\gamma} = s_\alpha(\boldsymbol{u}_1 - \boldsymbol{u}_2)\cdot\boldsymbol{s}$, measures the jump of the tangential velocity as one crosses the interface. It is the main quantity used to track interface positions and defines U and T in Eqs. (6) and (7). By using Darcy'law and the Young-Laplace equation, we calculate the distribution of vortex sheet in every time step by solving the following Fredholm integral equation

$$\tilde{\gamma} = 2As_\alpha \mathbf{W}\cdot\hat{s} + \frac{b^2\sigma}{6(\eta_1+\eta_2)}s_\alpha k_s. \tag{9}$$

This is an integral equation because the interface velocity, $\mathbf{W} = U\hat{n}+T\hat{s}$, is written as an integral of γ. In nondimensional terms, the distribution of vortex sheet is obtained from

$$\gamma = 2A\Re\left\{\frac{z_\alpha}{z} + \frac{z_\alpha}{2\pi \mathrm{i}}\mathrm{P}\int_0^{2\pi}\frac{\gamma(\alpha',t)}{z(\alpha,t)-z(\alpha',t)}d\alpha'\right\} + 2B\kappa_\alpha. \tag{10}$$

Here, s_α is the derivative of the arclength, s, with respect to the parameter, α, taken as the azimuthal angle; $z(\alpha,t) = x(\alpha,t)+iy(\alpha,t)$ denotes the complex position of the plane curve that describes the interface at a given instant of time, P expresses the principal value integral, and $\Re$ indicates the real part. Equation (10) was made dimensionless by taking the constant radius of the initial circle, R_0, as characteristic length, and $Q/(2\pi R_0)$ as characteristic velocity.

This equation presents the two dimensionless parameters that govern the dynamics. They are given by

$$A = \frac{\eta_1-\eta_2}{\eta_1+\eta_2} \quad \text{and} \quad B = \frac{\pi b^2\sigma}{6(\eta_1+\eta_2)QR_0}, \tag{11}$$

and represent the viscosity contrast and the effective surface tension, respectively.

System of Eqs. (6) and (7) require manipulation to arrive at the final version that will be discretized (Hou *et al.*, 1994, 2001). The normal velocity of the interface, U, depends on the integral of γ. This term can be written as the sum of two terms, one proportional to the Hilbert transform of γ,

$$H[\gamma] \equiv \frac{1}{\pi}\int_0^{2\pi}\frac{\gamma(\alpha')}{\alpha-\alpha'}d\alpha', \tag{12}$$

while the second becomes a smoothing operator. However, among the terms on the vortex sheet, γ, the one depending on curvature is the main source of stiffness. This realization motivates application of an implicit discretization method to this

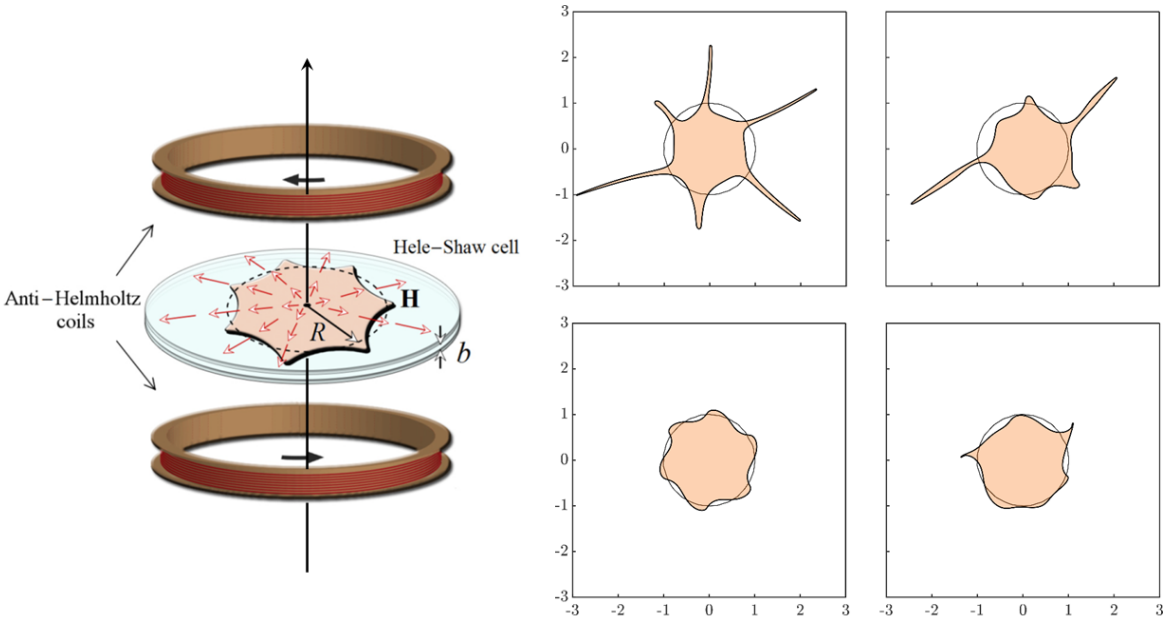

Figure 4. Ferrofluid interfacial patterns generated by the action of crossed magnetic fields generated by the superposition of the radial field and an azimuthal magnetic field produced by a current-carrying wire. The superposed influence of these fields induce a rotation of the droplet as deformations grow.

term only, i.e. $2B\kappa_\alpha = 2B\theta_{\alpha\alpha}/s_\alpha$, instead of to all terms of Eq. (10). To achieve that, we rewrite Eq. (7) as

$$\theta_t = B\left(\frac{2\pi}{L}\right)^3 H[\theta_{\alpha\alpha\alpha}] + \left\{\frac{2\pi}{L}U_\alpha - B\left(\frac{2\pi}{L}\right)^3 H[\theta_{\alpha\alpha\alpha}]\right\} + \frac{2\pi}{L}T\theta_\alpha. \tag{13}$$

Again, the terms inside curly brackets is a smoothing operator. To linearize this equation, we take advantage of the interesting property that the Hilbert transform diagonalizes under the Fourier transform, so the governing equations becomes

$$\hat{\theta}_t(k) = -\frac{B}{2}\left(\frac{2\pi}{L}\right)^3 |k|^3\hat{\theta}(k) + \hat{N}(k). \tag{14}$$

Here, the hat operator $\hat{}$ indicates Fourier transform, and $\hat{N}(k)$ contains all the terms the receive explicit treatment. They come from the terms inside the curly brackets and the last term in Eq. (13). The second governing equation, Eq. (6), can be simplified by making s_α constant so that $s_\alpha = L(t)/(2\pi)$, with L denoting the perimeter. This transforms the PDE into and ODE. With that, both equations can be integrated using Adams-Bashforth methods.

This description is focused on the viscous fingering instabilities that grow by the radial injection of a less viscous fluid to displace a more viscous one (Oliveira *et al.*, 2023) in a Hele-Shaw cell. The main modifications required in order to adapt this method to other displacement flows considered in this work is to update Darcy's law and calculate the appropriate form of the vortex sheet.

3. RESULTS

We present a few physical problems that have been addressed with the current methodology and show several interfacial patterns calculated with the boundary integral method based on the vortex sheet formalism. The discussion is brief so the emphasis is given to the methodology and to illustrations of how the approach can accurately capture intricate morphological patterns, some of them presenting sharp structures. Emphasis is given on sharpness because this usually derives from high gradients being of difficult numerical description. In addition, numerical integration can evolve the dynamics to very long times. To compensate for the lack of a richer physical discussion, we point the reader to published articles (Miranda and Alvarez-Lacalle, 2005; Oliveira and Miranda, 2020; Oliveira *et al.*, 2021, 2023).

Figure 1 shows ramified fingering structures formed when a less viscous fluid is injected at a constant flow rate for different values of the governing parameters that control the displacement flow. They are the viscosity contrast, A, and the effective surface tension, B, which is proportional to the inverse of a capillary number. The final times simulated are displayed by thick black contours and painted in the interior, while the internal gray curves mark intermediate time steps. Smaller A-values form larger stable radii where the resident fluid is completely displaced. Detailed discussion can be found in Oliveira *et al.* (2023).

Figure 2 shows interfacial patterns generated when the Hele-Shaw cell is rotated. The internal droplet is denser than the external fluid and instability is driven by centrifugal effects. Positive (negative) values of the viscosity contrast indicate that the internal (external) fluid is less (more) viscous. The effective surface tension B in this case compares the influence of interfacial tension and centrifugal effects. Larger values of this parameter have a stabilizing influence on pattern formation reducing the number of fingers. Detailed discussion can be found in Miranda and Alvarez-Lacalle (2005).

Figure 3 presents results from the radial stretching of a magnetic droplet by the action of a magnetic field generated by two coils in the anti-Helmholtz configuration, i.e., in which the electric current runs in opposite directions. Ferrofluids are stable colloidal suspension of nanometersized magnetic particles and keept a Newtonian viscosity. Magnetorheological (MR) fluids have larger, micronsized magnetic particles in their composition. This renders the fluid viscoelastic properties in the form of a magnetic field dependent yield stress. The radial field tends to spread the droplet radially, while surface tension stabilizes interfacial deformations. The presence of yield stress further stabilizes interfacial perturbations, and the patterns obtained with the MR fluid have less ramifications and retain for more fluid next to the origin. Detailed discussion for ferrofluid deformations under the influence of the radial field can be found in Oliveira and Miranda (2020). Results for the MR fluids are preliminary.

Magnetic materials are very sensitive to the applied magnetic field. So, simple changes in the field configuration leads to different droplet dynamics. For a ferrofluid, Figure 4 considers the influence of two magnetic fields, the radial one superposed to an azimuthal field generated by a current-carrying wire. The resulting interfacial patterns still grow radially, but are skewed. In addition, the entire pattern rotates according to the sign of the electric field. If the droplet is more viscous than the external fluid and stable with regard to Saffman-Taylor instability (left column), and if the droplet is subjected to mild field intensities (larger B values on bottom row), then interfacial patterns achieve a steady, symmetrical shape becoming insensitive to the initial random perturbation. Detailed discussion can be found in Oliveira *et al.* (2021).

4. CONCLUSIONS

We have implemented and described a boundary integral method based on the vortex sheet formalism to track deformations between fluids of different viscosities whose interface is governed by surface tension. This is a very powerful numerical technique with spectral accuracy that reduces the two-dimensional unstable displacement flow to an one-dimensional problem by describing interface deformations as a closed planar curve. The technique as been applied to describe: (i) the growth of Saffman-Taylor fingers in radial displacements (Oliveira *et al.*, 2023); (ii) centrifully spreading droplets confined in the Hele-Shaw cells (Miranda and Alvarez-Lacalle, 2005); and deformations of magnetic droplets subjected to different magnetic field configurations (Oliveira and Miranda, 2020; Oliveira *et al.*, 2021).

5. REFERENCES

Abedi, B., Berghe, L.S., Fonseca, B.S., Rodrigues, E.C., Oliveira, R.M. and de Souza Mendes, P.R., 2022. "Influence of wall slip in the radial displacement of a yield strength material in a hele-shaw cell". *Phys. Fluids*, , No. 113102.

Alvarez-Lacalle, E., Ortin, J. and Casademunt, J., 2006. "Relevance of dynamic wetting in viscous fingering patterns". *Phys. Rev. E*, Vol. 74, No. 025302(R).

Casademunt, J., 2004. "Viscous fingering as a paradigm of interfacial pattern formation: Recent results and new challenges". *Chaos*, Vol. 14, No. 3, pp. 809–824.

Ceniceros, H.D., Hou, T.Y. and Si, H., 1999. "Numerical study of hele-shaw flow with suction". *Phys. Fluids*, Vol. 11, No. 9.

Homsy, G.M., 1987. "Viscous fingering in porous media". *Annu. Rev. Fluid Mech.*, Vol. 19, pp. 271–311.

Hou, T.Y., Lowengrub, J.S. and Shelley, M., 1994. "Removing the stiffness from interfacial flows with surface tension". *J. Comput. Phys.*, Vol. 114, pp. 312–338.

Hou, T.Y., Lowengrub, J.S. and Shelley, M., 2001. "Boundary integral methods for multicomponent fluids and multiphase materials". *J. Comput. Phys.*, Vol. 169, pp. 302–362.

McCould, K.V. and Maher, J.V., 1995. "Experimental perturbations to saffman-taylor flow". *Phys. Rep.*, Vol. 260, pp. 139–185.

Miranda, J.A. and Alvarez-Lacalle, E., 2005. "Viscosity contrast effects on fingering formation in rotating hele-shaw flows". *Phys. Rev. E*, Vol. 72, No. 026306.

Morrow, L.C., Moroney, T.J. and McCue, S.W., 2019. "Numerical investigation of controlling interfacial instabilities in non-standard hele-shaw configurations". *J. Fluid Mech.*, Vol. 877, pp. 1063–1097.

Oliveira, R.M., Coutinho, I.M., Anjos, P.H.A. and Miranda, J.A., 2021. "Shape instabilities in confined ferrofluids under crossed magnetic fields". *Phys. Rev. E*, Vol. 104, No. 065113.

Oliveira, R.M. and Miranda, J.A., 2020. "Fully nonlinear simulations of ferrofluid patterns in a radial magnetic field". *Phys. Rev. Fluids*, Vol. 5, No. 124003.

Oliveira, R.M., Abedi, B., Santos, L.F., Câmara, P.S. and de Souza Mendes, P.R., 2023. "Similarity characteristics in the

morphology of radial viscous fingers". *Phys. Fluids*, , No. 042114.

Saffman, P.G. and Taylor, G.I., 1958. "The penetration of a fluid into a porous medium or Hele-Shaw cell containing a more viscous liquid". *Proc. R. Soc. London. Ser. A*, Vol. 245, No. 1242, pp. 312–329.

Zhao, M., Anjos, P.H.A., Lowengrub, J. and Li, S., 2020. "Pattern formation of the three-layer Saffman-Taylor problem in a radial Hele-Shaw cell". *Phys. Rev. Fluids*, Vol. 5, No. 124005.

6. RESPONSIBILITY NOTICE

The author is solely responsible for the printed material included in this paper.